Infrasonic wind-noise reduction by barriers and spatial filters

Michael A. H. Hedlin[a)]
Institute of Geophysics and Planetary Physics, Scripps Institution of Oceanography, University of California, San Diego, La Jolla, California 92093-0225

Richard Raspet
National Center for Physical Acoustics, University of Mississippi, University, Mississippi 38677

(Received 2 October 2002; revised 10 June 2003; accepted 12 June 2003)

This paper reports experimental observations of wind speed and infrasonic noise reduction inside a wind barrier. The barrier is compared with ''rosette'' spatial filters and with a reference site that uses no noise reduction system. The barrier is investigated for use at International Monitoring System (IMS) infrasound array sites where spatially extensive noise-reducing systems cannot be used because of a shortage of suitable land. Wind speed inside a 2-m-high 50%-porous hexagonal barrier coated with a fine wire mesh is reduced from ambient levels by 90%. If the infrasound wind-noise level reductions are all plotted versus the reduced frequency given by f^*L/v, where L is the characteristic size of the array or barrier, f is the frequency, and v is the wind speed, the reductions at different wind speeds are observed to collapse into a single curve for each wind-noise reduction method. The reductions are minimal below a reduced frequency of 0.3 to 1, depending on the device, then spatial averaging over the turbulence structure leads to increased reduction. Above the reduced corner frequency, the barrier reduces infrasonic noise by up to 20 to 25 dB. Below the corner frequency the barrier displays a small reduction of about 4 dB. The rosettes display no reduction below the corner frequency. One other advantage of the wind barrier over rosette spatial filters is that the signal recorded inside the barrier enters the microbarometer from free air and is not integrated, possibly out of phase, after propagation through a system of narrow pipes. [DOI: 10.1121/1.1598198]

PACS numbers: 43.28.Dm, 43.28.We [LCS]

I. INTRODUCTION

A. Air flow and infrasonic noise

It is well known that a direct scaling relationship exists between air flow and acoustic noise in the atmosphere. The inverse relationship between pressure and velocity for a nonviscous fluid with steady flow is given by Bernoulli's principle

$$p+(\rho v^2)/2+\rho g h=C, \tag{1}$$

where p is pressure, ρ is density, v is wind velocity, g is the acceleration due to gravity, h is the height, and C is a constant. Velocity and pressure are inversely related if h is held constant and if energy is conserved. Differentiation of this formula, with ρ and h held constant, shows the simplicity of this scaling

$$\delta p \sim \rho v\, \delta v. \tag{2}$$

Morgan and Raspet (1992) measured the incoming wind speed and wind fluctuation on a microphone and demonstrated that the pressure fluctuations obey Eq. (2) within a constant factor ranging from 1.1 to 1.6. Much of the acoustic noise at short periods is due to turbules that are carried past the recording site, or advected, by ambient wind (Grover, 1971) with the frequency band of the noise governed largely by the scale of the turbules (McDonald, Douze, and Herrin, 1971) and, as we will show later, by the wind speed. Strasberg has discussed the physical mechanisms of infrasonic flow noise underwater as measured by hydrophones (Strasberg, 1979) and has applied this analysis to develop scaling laws for microphone wind screens in nonturbulent flows (Strasberg, 1988). Other sources of acoustic noise in the atmosphere are not directly related to the flow of air at the observation point, but are due to buoyancy waves and larger scale convective activity in the atmosphere (Priestley, 1966; Gossard and Hooke, 1975). The frequency dependence of this noise is governed by the spatial structure of turbulence in the atmosphere in the vicinity of the point where the noise is being measured. In general terms, atmospheric turbulence is concentrated near Earth's surface in the atmospheric boundary layer (ABL; Kaimal and Finnigan, 1994). The upper extent of the ABL is highest (1 to 2 km) during the day when the Earth's surface radiates heat and lowest (tens of meters) or nonexistent during the night (Panofsky and Dutton, 1984; Kaimal and Finnigan, 1994). Wind shear introduces smaller eddies and ''cascades'' energy from the low to the higher frequencies (Kaimal and Finnigan, 1994).

B. The new global infrasound monitoring network

The tabling of the Comprehensive nuclear Test-Ban Treaty (CTBT) at the United Nations in September, 1996 increased interest in monitoring globally for nuclear tests at all explosive yields. The treaty comes with an International Monitoring System (IMS), which will include networks of seismic, infrasonic, hydro-acoustic, and radionuclide stations. This paper relates to the infrasound component of the

a)Electronic mail: hedlin@ucsd.edu

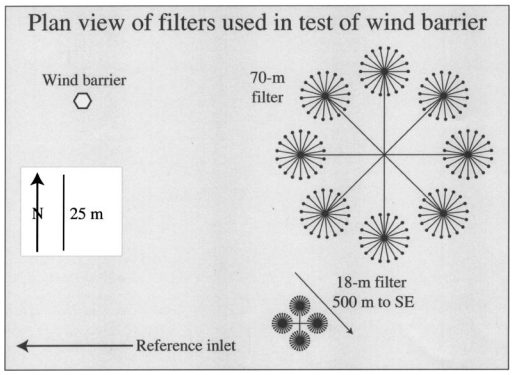

FIG. 1. Plan view of all filters tested in this experiment. The 70- and 18-m rosette filters are part of the International Monitoring System (IMS) array I57US. The 18-m filter is located 500 m to the southeast of the main study area. The large rosette filter comprises 144 low-impedance inlets distributed across an area 70 m in diameter. The small rosette filter comprises 96 low-impedance inlets distributed across an area 18 m in diameter. These filters are described in more detail in Alcoverro (1998) and Hedlin *et al.* (2003). All filters are shown to scale.

IMS. The infrasound network will comprise 60 arrays distributed globally. Each array will include up to eight sensors. The dynamic atmosphere is inherently noisy at frequencies of interest to the nuclear monitoring community (between 0.01 and 8 Hz). As a result, it is necessary to suppress ambient infrasonic noise at each station in the infrasound network. IMS stations are currently being equipped with ''rosette'' spatial noise reduction systems (Fig. 1; Alcoverro, 1998; Hedlin, Alcoverro, and D'Spain, 2003). To achieve a spatially uniform global network, 23 of the stations are located on oceanic islands.

C. Rationale for the present study

As development of the IMS global infrasound network progresses, and given that little suitable land is available at some of the sites, there is a pressing need for effective, spatially compact, passive infrasonic noise-reducing devices. An intercomparison of the noise-reducing systems currently deployed at new IMS infrasound array sites and spatially compact systems, such as the wind barrier, has not yet been done. Grover (1971) compared very small wind screens (<1 m high) with pipe filters that are not still in use. This paper reports an intercomparison of a small, 2-meter-high, wind- and noise-reducing barrier with large spatial filters that are currently in use at IMS infrasound array sites. Noise levels inside the barrier are also compared with ambient noise levels to gauge, in an absolute sense, the utility of the barrier for reducing infrasonic noise across the frequency band of interest to the nuclear monitoring community. The physics underlying interest in the wind barrier is straightforward. Noise scales with wind, and therefore reducing wind, and fragmenting advected turbules, at the site of the microbarometer should lead to lower noise levels and an improved ratio of signal to noise. The microbarometer we used in our experiment is described later in the paper (Sec. II E). This paper seeks answers to three questions: (1) What is the frequency band over which a wind barrier reduces noise? (2) By how much is the noise reduced in this band? And (3) Does the barrier compare favorably with spatial filters as a system for preserving signals of interest while attenuating noise?

II. EXPERIMENT LAYOUT

A. The infrasound test-bed

The experiment was conducted at the Cecil H. and Ida M. Green Pinon Flat Observatory in the Anza-Borrego desert in southern California during a 40-day interval in August and September of 2000. The Pinon Flat Observatory is useful for studies of infrasonic noise-reducing systems as wind speeds in this area range from near zero at night to somewhat above 10 m/s during the day. In addition to strong diurnal variations in meteorological conditions, the area experiences significant seasonal variations. The infrasonic noise levels scale directly with wind speed (McDonald, Douze, and Herrin, 1971; Hedlin, Alcoverro, and D'Spain, 2003). A diagram showing the design of the spatial filters we compared with the wind barrier and the relative locations of all filters used in our study is given in Fig. 1.

B. Design considerations for the wind barrier

The design of the wind barrier used in this experiment was guided partly by previous work by Lizska, and by Bernoulli's scaling between wind speed and pressure. The barrier chosen for this site is 2 m tall and 5.5 m across at the base. To avoid increasing large-scale turbulence downstream of the barrier, we followed Lizska and used a barrier that was 50% porous on the sides. As shown in Fig. 2, the openings in the hexagonal barrier are horizontal. The barrier was coated with a fine mesh to further decrease wind flow inside. The wire mesh used had square openings 1 mm on a side. As we see later, the observed reduction in infrasonic noise does not scale as expected with the reduction in wind speed, pointing to a different mechanism for noise reduction inside the barrier that relies on averaging pressure variations across the surface of the barrier and not directly on the reduction of wind speed at the microbarometer inside the barrier.

To test the wind barrier, infrasonic noise and meteorological data were collected at four sites. A microbarometer and a wind sensor were located inside the hexagonal wind barrier (Fig. 2) at a height of 60 cm. The other sensors were located at the sites described in the following sections.

C. Rosette spatial filters

The second and third sensors were attached to 18- and 70-m-diameter ''rosette'' spatial noise-reducing filters at the nearby IMS infrasound array I57US (Fig. 1). The rosette filters comprise a number of low-impedance inlets distributed across a circular area (Alcoverro, 1998; Hedlin, Alcoverro, and D'Spain, 2003). Atmospheric noise from local sources is known to be incoherent at offsets of several meters or less, while signals from remote sources can be coherent at distances of hundreds of meters (Priestley, 1966). Pressure variations sampled by N inlets are summed, with signal-to-noise levels improved by $N^{1/2}$ at sites where the noise is uncorrelated between the inlets (Daniels, 1959). The rosettes provide spatial averaging over the local turbulent structures.

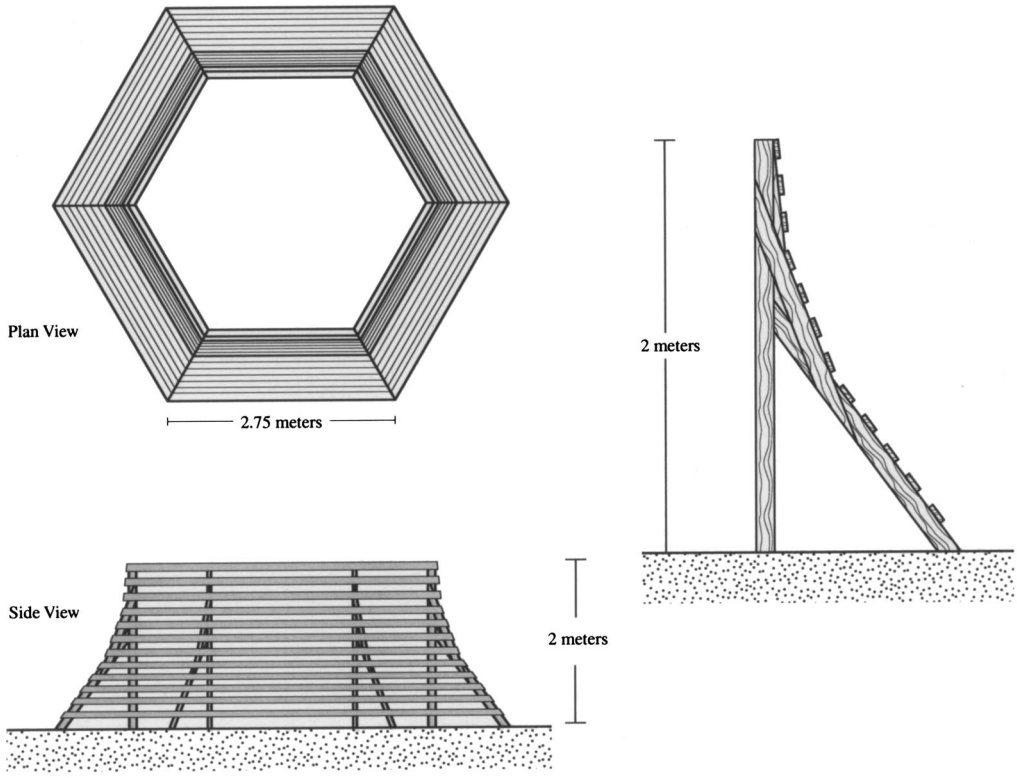

FIG. 2. The wind barrier considered in this paper consists of six sides, each 2 m tall. The barrier is not solid on the sides, as theory indicates this would increase turbulence and infrasonic noise. The sides of the barrier are 50% porous (i.e., one half solid). Additional high-frequency noise reduction was achieved by coating the sides of the barrier with a fine wire mesh similar to residential bug screens. The top of the barrier was just coated with the wire mesh but otherwise uncovered. The design of our barrier was suggested by Ludwik Liszka. Exact specifications were given by Doug Revelle (Los Alamos National Laboratory). The MB2000 sensor was located in foam within a porous aluminum shell at an elevation of 60 cm at the center of the barrier. The foam provided additional reduction of high-frequency noise; the shell protected the sensor from the elements. This barrier was patented by Liszka in 1975 (Liszka, L.: Swedish Patent No. 7315138-3, October 30, 1975). The drawing in this figure was taken from this patent document.

D. Reference noise measurements

To allow us to gauge the utility of the wind barrier at reducing infrasonic noise from ambient levels, all recordings inside the wind barrier were made concurrently with recordings made at the fourth site equipped with no noise-reducing system. At the reference site, one sensor was attached to a single, low-impedance inlet located 5 cm above the ground. See Fig. 3.

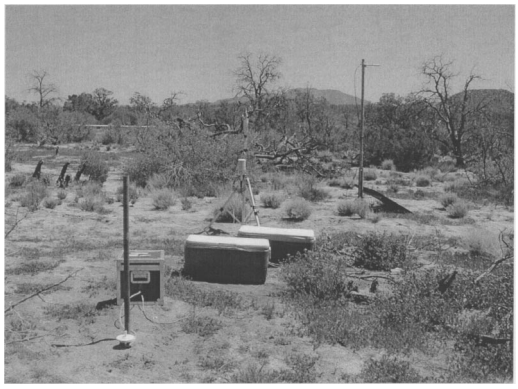

FIG. 3. Photo of reference site. The low-impedance inlet is located 5 cm above the ground. The microbarometer is located in a case immediately behind the inlet. The recording equipment and power system are located to the right of the microbarometer. The wind and temperature sensors are located 2 m and 1 m above the ground immediately behind the recording equipment. The radio antenna is located to the far right.

E. Recording system

Infrasonic pressure data were collected at all four sites located within an area 150 m across. No sites were located downwind from the barrier to avoid artificial sheltering from the wind. All pressure data were collected with MB2000 aneroid microbarometers. The sensors were fabricated by the French Dépertement Analyse et Surveillance de l'Environnement (DASE). The MB2000 sensor filters the signal between 0.01 and 27 Hz. The recording system filters the data below 9 Hz to avoid aliasing. Pressure data were sampled at all sites at 20 Hz. Meteorological data (wind speed, direction, air temperature, and humidity) were sampled at all four sites at 1 Hz. All data were digitized by 24-bit Reftek dataloggers and transmitted in real time via 2.2-GHz telemetry link to our laboratory in La Jolla. Power for all equipment was provided via solar panels and batteries.

III. EXPERIMENTAL RESULTS

The core of the observational work has been the spectral analysis of segments of infrasonic and meteorological data that were collected simultaneously by identical microbarometers attached to different noise-reduction systems—or to no noise-reduction device at all. The data analysis is based on 15-min segments of data taken from nonoverlapping intervals throughout the experiment. Every hour, four segments of data were selected for further analysis. A segment was

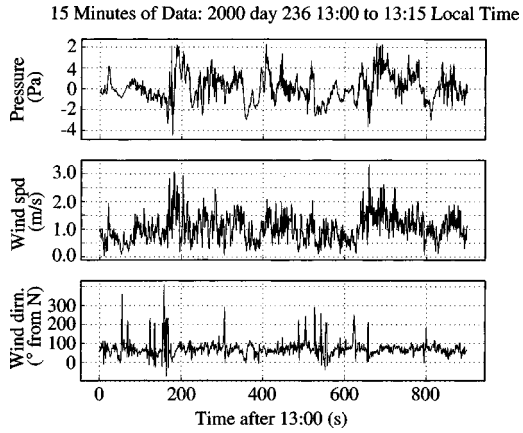

FIG. 4. Atmospheric pressure and meteorological data from a 15-min interval starting at 13:00 GMT on day 236 of 2000 at the reference site. Filtered pressure data are shown in the upper panel. Wind speed and direction are shown below.

removed from consideration only if data were lost during that time interval at any of the four sites. The results presented in this paper came from 40 days of observations and involve a total of 3074 spectral estimates and over 3 million observations of wind velocity at each site. One example of infrasonic pressure and meteorological data is given in Fig. 4. This figure presents a typical 15-min segment of data collected inside the wind barrier. During the entire experiment, the wind speed varied from near zero to above 10.0 m/s.

A. Wind-speed reduction

Figure 5 shows the effectiveness of the wind barrier at reducing the wind speed. The test of wind reduction occurred in two phases. In both phases, wind speed was measured at the center of the barrier at a height of 60 cm and outside at a height of 2 m at the location of the reference inlet. In the first phase, a 50% porous wind barrier was used. In the second phase, the sides and top of the barrier were coated with a fine wire mesh. The mesh is composed of a Cartesian grid of wires spaced by 1 mm. The histograms in the lower panel of Fig. 5 show the number of wind-speed observations made as a function of ambient wind speed (i.e., wind speed recorded outside the barrier at the reference site). To calculate each histogram, the wind-speed data at the reference site were binned into intervals spanning 0.1 m/s. Most observations from both phases of the experiment were made at wind speeds below 2.0 m/s. The winds were slightly stronger during the phase of the experiment when the barrier was coated with a mesh. The upper panel displays the average wind speed observed inside the barrier and the ambient wind speed recorded at the reference site. To calculate the average as a function of wind speed, individual observations were binned as described above. Each average was calculated from simultaneous observations made inside the barrier and at the reference site. A barrier that provided no shielding from the wind would yield a curve lying along the dashed line. The data show that the uncoated barrier reduces the wind speed by ~80% at times when the unsuppressed wind speed exceeded 10 m/s. The addition of the wire mesh increased the wind reduction to 90%.

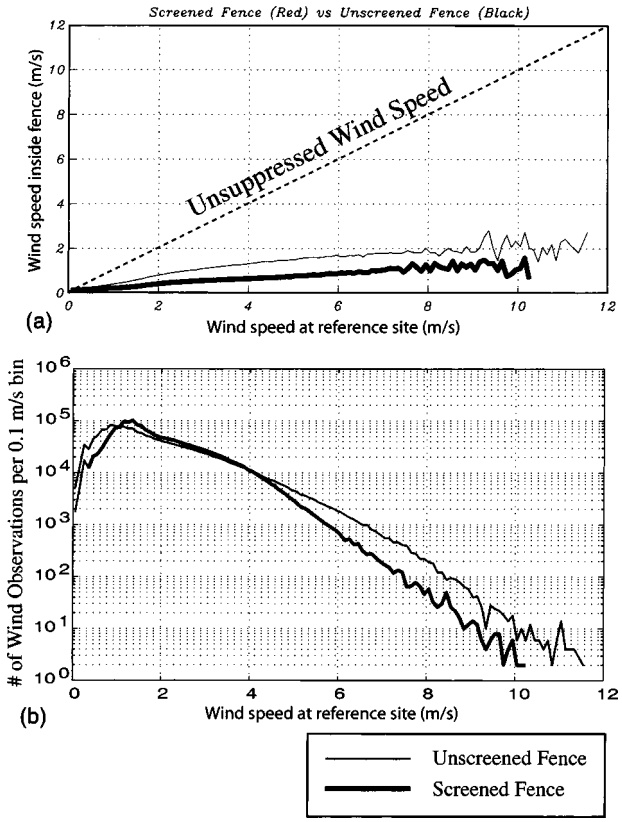

FIG. 5. Data collected by anemometers at a height of 60 cm within the wind barrier and outside at a height of 2 m indicates that the barrier is highly effective at reducing wind speed. The lower panel shows the number of observations at the reference site as a function of wind speed. This figure is based on a total of 3.3 million wind-speed observations (made once/second). The faint curve represents data collected before the wind barrier was coated with a wire mesh. The dark curve represents data collected after the sides of the wind barrier were coated with the mesh. The upper panel compares the wind speed inside the barrier to that observed outside. If the wind barrier was completely ineffective at reducing wind speed, the data would lie along the dashed line. The 50%, uncoated, wind barrier reduces wind speed by ~80%. The addition of the mesh reduces wind speed further to 90%. As shown in panel (b), the ambient wind speeds were slighly higher during the test of the barrier with the external mesh. It must also be noted that because the wind sensor inside the barrier was closer to the ground than the sensor outside at the reference site (60 cm vs 2.0 m), some wind-speed reduction would be expected even in the absence of a wind barrier. A separate experiment indicated that average wind speeds at the observatory at a height of 60 cm are 60% of the wind speeds at 2.0 m.

B. Noise reduction

Although the wind barrier provided substantial shielding from the wind, the main objective of this paper is to judge the effectiveness of the barrier at reducing infrasonic noise. Figure 6 summarizes this result. Given that individual power spectral estimates are inherently noisy, the analysis is based on stacked spectra. In this analysis, each of the 3074 spectral estimates is associated with a single wind-speed value and is binned by that value. The wind-speed value associated with an individual power spectral estimate is the average wind speed at the reference site from the 15-min time interval spanned by the spectral estimate. The wind-speed bins used in this analysis spanned 0.5 m/s, starting at 0.0 m/s. Each panel in Fig. 6 displays stacked power spectral estimates from each of the four sites. For example, the upper-left panel shows in black the average ambient noise levels when the

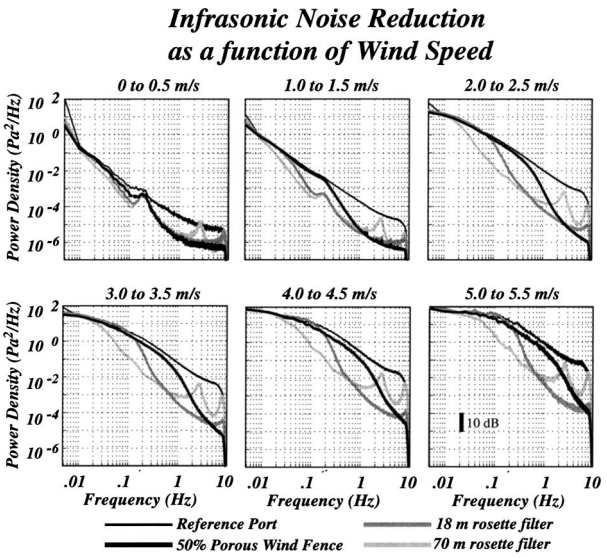

FIG. 6. Due to high variance in individual power spectral estimates, individual estimates are grouped by wind speed and stacked to provide a clearer view of the utility of the wind barrier at reducing infrasonic noise and the dependence of infrasonic noise as a function of wind speed and frequency. Stacked power spectral density estimates taken from data collected at four sites over a 40-day interval are shown at wind speeds ranging from <0.5 m/s to above 5.0 m/s. Ambient noise levels are indicated by the black curves in each panel. Data collected inside the 50%-porous, screened, wind barrier are represented by the thick black curves. For reference, data collected via ''rosette'' filters at a nearby IMS infrasound array (I57US) are also shown. Data collected via a 70-m aperture rosette filter are shown in light gray. The thin black curves represent data collected via a single reference inlet. Data from a 18-m rosette filter are shown in heavy gray. The rosette filters are described in more detail by Alcoverro (1998) and Hedlin, Alcoverro, and D'Spain (2003). The stacked spectra reveal the increase in infrasonic noise with decreasing frequency at all wind speeds. Noise levels increase with increasing wind speed at all frequencies; however, the greatest increase in noise levels occurs at high frequencies. The screened wind barrier provides noise suppression at high frequencies. The corner frequency of the filter increases with increasing wind speed from $\sim$0.2 Hz at wind speeds below 0.5 m/s to $\sim$1.0 Hz at wind speeds above 5.0 m/s. All wind data used in this figure were collected at a height of 2.0 m at the reference inlet. In total, 3074 15-min intervals of data were used in this figure. Each interval provided a single power spectral density estimate and a single wind-speed value determined by taking an average of all wind-speed measurements made during the 15 min covered by the spectral estimate.

wind speed at the reference site was below 0.5 m/s. The noise levels observed in the barrier, at the 70-m rosette and the 18-m rosette filter are shown in black, light-, and dark gray, respectively. This figure shows the growth of infrasonic noise at all sites with increasing wind speed and with decreasing frequency. More importantly for this study, this figure shows the relative utility of the different systems.

The frequency band over which the barrier is effective scales with wind speed. At high frequencies, the screened 50%-porous wind barrier reduces infrasonic noise by 20 to 25 dB and is superior to the spatial filters at frequencies above 1 to 5 Hz, with the greatest advantage observed at low wind speeds. The wind barrier is less effective than the spatial filters at reducing infrasonic noise at all wind speeds at frequencies below 1–2 Hz. The barrier offers 0- to 5-dB noise reduction at frequencies below 1 Hz. Resonance is observed in data from the rosette filter at frequencies above 0.7 Hz (Fig. 6; Hedlin, Alcoverro, and D'Spain, 2003). The microbarom peak is observed inside the wind barrier only under calm conditions.

IV. FREQUENCY DEPENDENCE OF THE WIND NOISE REDUCTION

Figure 7 displays the wind-noise reduction versus scaled frequency fL/v, where f is the frequency, L the device scale size, and ν the average wind speed for the three highest wind speeds. In this plot, the diameters of the rosettes and wind barrier are used (18, 70, and 5.5 m). The diameter of the wind barrier is the distance at ground level between opposite sides. Each set of data is offset by a factor of 100.

If the wind noise and wind-noise reduction are caused by local interactions of the turbulence and the wind-noise reduction device, the wind-noise reductions of similar devices should scale as the ratio of the turbulence scale to a characteristic linear dimension of the device (Strasberg, 1988). The turbulence size corresponding to a given frequency is given by the average wind speed divided by the frequency. Thus, Fig. 7 displays the relative effectiveness of a device weighted by its size.

The behavior of the reduction versus scaled frequency for each wind speed is very similar. The contribution from the resonance in the 70-m rosette does not scale with wind speed, but the other features do. The two rosettes are effective at spatially averaging the turbulent pressure fluctuations if the scaled frequency is greater than 1. There are minor differences between the 18- and 70-m rosette, but the scaling appears to hold well in general. The wind barrier appears to roll off at a higher scaled frequency, indicating that the spatial averaging is occurring over a smaller region. Reasonable agreement between the roll-off frequency of the rosettes and the wind barrier can be obtained by using the barrier height as the averaging scale. This is presented in Fig. 8 along with additional data from spherical wind screens which will be discussed in Sec. V. In Fig. 8 it can be observed that the wind barrier produces a small but significant 4-dB reduction for scaled frequencies between 0.05 and 0.5.

V. DISCUSSION

The data presented above display several unexpected results. A reduction in wind speed inside the barrier by a factor of 10 does not result in a proportional reduction in infrasonic wind-noise power by a factor of 100. Second, the wind-noise reduction by the barrier scales much like the wind-noise reduction of the rosettes produced by spatial averaging. The appropriate size for scaling of the barrier appears closer to the height of the barrier, 2.0 m, rather than the diameter, 5.5 m. The barrier does display a small but significant reduction even when the size of the turbulence is greater than the size of the barrier itself. On the scaled plot, assuming the effective size of the barrier is 2 m, the infrasonic spectrum is reduced by a factor of 1/(2.5), or by -4 dB over the scaled frequency range of 0.05 to 0.5.

Some insight into the mechanism for this reduction can be gained by a study of the literature of wind-noise reduction at audio frequencies. Phelps (1938) suggested that the mechanism for wind-noise reduction for low frequencies is

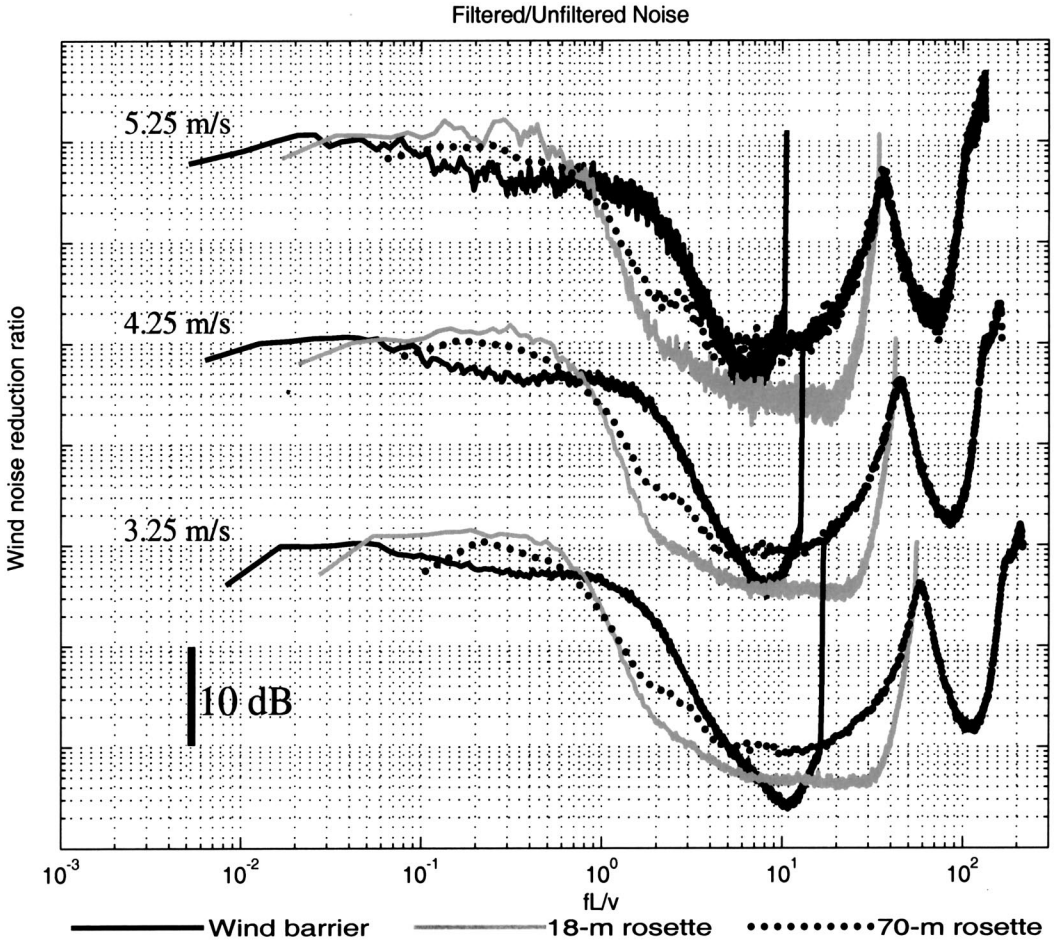

FIG. 7. Wind-noise reduction versus scaled frequency at 3.25, 4.25, and 5.25 m/s for the 70-m rosette (bold dots), the 18-m rosette (bold gray), and the 5.5-m wind barrier (black curves).

as follows: the pressure profile induced by the wind over a spherical screen has regions of high and low pressure. Since the pressure fluctuations in incompressible flows are governed by the Laplace equation in regions of little or no flow (inside the screen), the pressure at the microphone can be calculated by area averaging over the screen surface. Phelps used the equations for the pressure distribution for steady inviscid incompressible flow over a rigid sphere to demonstrate a predicted reduction of 6.0 dB for turbulence scales larger than the size of the windscreen. The pressure distribution around a rigid sphere is dominated by a strong low-pressure region behind the wind screen. Morgan measured the pressure distribution around 90- and 180-mm diameter spherical foam windscreens and used the measured data to evaluate the reduction (Morgan, 1992). He found that the small flow through the porous windscreen leads to a smaller low-pressure region behind the wind screen and therefore a smaller average pressure. He arrived at a value of 14 dB (0.04 relative power) for this reduction. Data from Morgan's dissertation for the wind-noise reduction of a 90- and 180-mm screen for 4.84- and 4.74-m/s wind speeds in the frequency bands from 1.6 to 500 Hz are also displayed in Fig. 8, where the characteristic length dimension corresponds to the diameter of the spherical windscreen. At small scale sizes, the data agree reasonably well with the prediction of 14 dB. The reductions are not constant but vary slowly up to scale screen sizes of 0.3. As the scale size increases beyond 0.3, additional reduction occurs since different portions of the screen are now sensing different turbulent structures. This averaging is comparable to the averaging by the rosettes. The reduction in the low-pressure region behind the screen due to flow-through also reduces the intensity of wake turbulence and displaces the onset of turbulence further from the screen (Schomer *et al.*, 1990).

It appears that the wind barrier may be acting somewhat like a foam windscreen in that it does display reductions in wind-noise intensity even when the turbulence structures are larger than the screen. The reductions are not as large as displayed for the spherical foam windscreens since the top of the barrier is open. In addition, the pressure distribution is not known and may be far from optimal since the pressure-averaging mechanism was not considered in the barrier design.

VI. CONCLUDING REMARKS

A. Wind-noise reduction

Comparison of the scaled reductions in wind noise produced by the rosettes and wind barrier with the reductions afforded by a spherical windscreen hold promise for significant wind-noise reduction with a smaller footprint device. The rosettes only produce reductions if the scale size of the

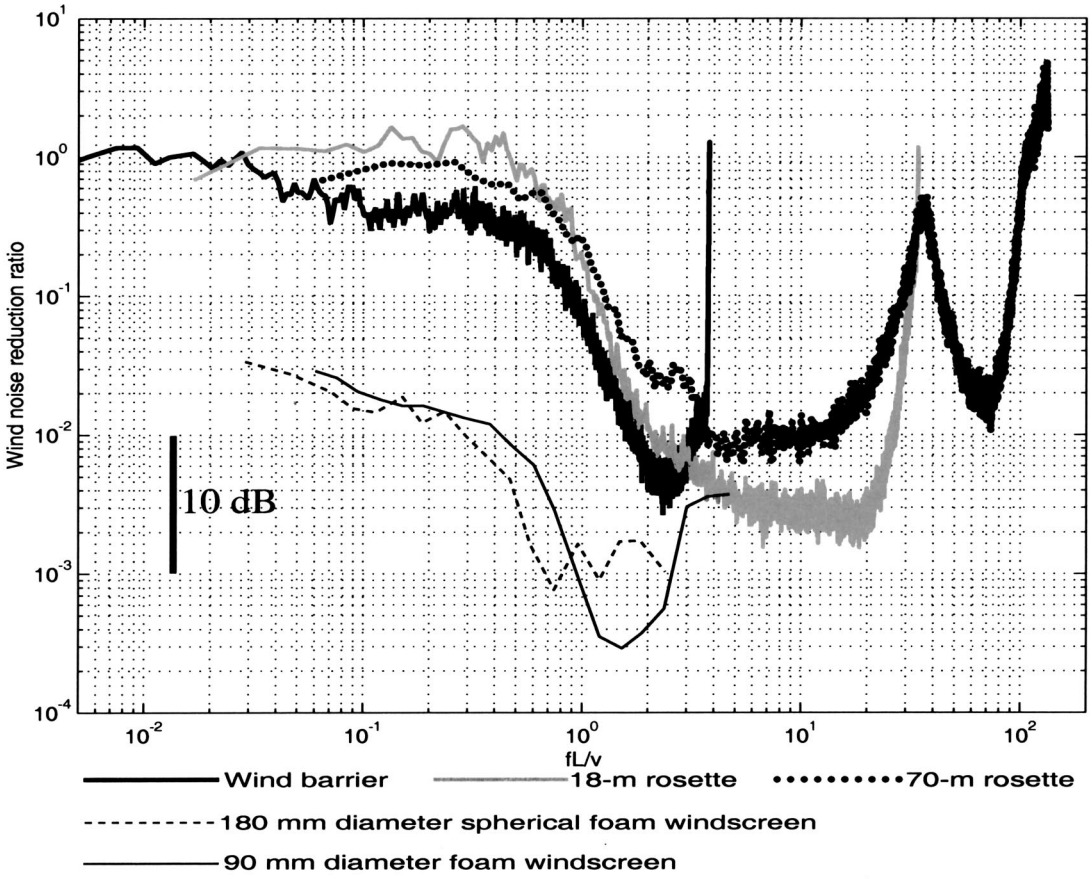

FIG. 8. Wind-noise reduction versus scaled frequency at 5.25 m/s for the 70-m rosette (bold dots), for the 18-m rosette (bold gray). and for the wind barrier (bold black) using the height of 2.0 m to calculate the scaled frequency. Also displayed is the noise reduction produced by a 90-mm-diameter foam windscreen at an average wind speed of 4.84 m/s (light dashed curve) and a 180-mm diameter spherical foam wind screen at 4.74 m/s (light solid curve).

turbulence is smaller than the size of the rosette, since such devices rely on the incoherence of the turbulence at each inlet. The wind barrier displayed large reductions only when the scale size of the turbulence is smaller than the height of the barrier. However, a reduction of about 4.0 dB was achieved by the wind barrier for turbulence scales up to 20 times the barrier height (reduced frequencies down to 0.05). This reduction may be due to a mechanism similar to that of the spherical foam windscreens. In the spherical windscreens, these reductions occur since the pressure measured at the center is the area average of the pressures generated at the surface of the sphere. For large turbules, the pressure generated by an increase in wind speed is positive at the front and negative at the back, and the average is less than the pressure fluctuation measured at a bare sensor. The wind barrier may serve as a pressure averaging device over the surface of the barrier with negative and positive contributions even for turbulent structures with dimensions much larger than the windscreen.

The similarity of the results of the wind barrier and the spherical foam ball suggest that a wind-barrier design based on the principle of spherical windscreen reduction may produce a more effective, more compact infrasonic wind-noise reduction device.

B. Preserving signals while attenuating noise

Ultimately, we seek a device that will provide maximum attenuation of unwanted noise and minimally distorted recordings of signals from remote sources. Signals and noise are received at a single point inside the barrier. This is potentially a significant advantage of the barrier over spatial filters, such as the two considered in this paper, which rely on the different coherence lengths of signal and noise. Spatial filters are used to increase the ratio of signal to noise by sampling air pressure at numerous locations at offsets at which the noise is believed to be incoherent and the signal remains coherent. If phasing between the multiple samples of the signal is not correctly taken into account, and if the signal is not coherent across the area spanned by the spatial filter, the waveform of the signal will be degraded. Rosette filters are tuned to signals arriving with infinite phase velocity. Signal attenuation caused by 70-m aperture rosette filters becomes acute at low angles of incidence and at frequencies above 1 Hz (Hedlin, Alcoverro, and D'Spain, 2003).

Unlike spatial filters currently in use at IMS array sites, the barrier does not propagate the signals through narrow pipes. Ambient signal and noise enter the microbarometer from free air and therefore, dispersion of broadband signals that is known to occur in narrow pipes (e.g., Benade, 1968) is not a concern.

ACKNOWLEDGMENTS

Pioneering work on the wind barrier by Ludwik Liszka (Swedish Institute of Space Physics) made this research possible. The design of the wind barrier and insights into how

the barrier reduces infrasonic noise were provided by Doug Revelle (Los Alamos National Laboratory). David Revelle constructed the barrier. We thank Hank Bass (University of Mississippi), Lou Sutherland (the associate editor), and two anonymous reviewers for constructive comments on the manuscript. Frank Vernon, Jennifer Eakins, and Glen Offield provided the real-time data link. Clint Coon provided field assistance. Funding was provided by the Defense Threat Reduction Agency under Contract No. DTRA01-00-C-0085.

Alcoverro, B. (**1998**). ''Acoustic filters design and experimental results,'' in Proceedings: Workshop on Infrasound, Commissariat à l'Energie Atomique, Bruyères-le-Châtel, France, 21–24 July 1998.

Benade, A. H. (**1968**). ''On the propagation of sound waves in a cylindrical conduit,'' J. Acoust. Soc. Am. **44**, 616–623.

Burridge, R. (**1971**). ''The acoustics of pipe arrays,'' Geophys. J. R. Astron. Soc. **26**, 53–69.

Daniels, F. P. (**1959**). ''Noise reducing line microphone for frequencies below 1 cps,'' J. Acoust. Soc. Am. **31**, 529–531.

Grover, F. H. (**1971**). ''Experimental noise reducers for an active microbarograph array,'' Geophys. J. R. Astron. Soc. **26**, 41–52.

Gossard, E. E., and Hooke, W. H. (**1975**). *Waves in the Atmosphere* (Elsevier Scientific, New York).

Hedlin, M. A. H., Berger, J., and Vernon, F. L. (**2002**). ''Surveying infrasonic noise on oceanic islands,'' Pure Appl. Geophys. **159**, No. 5, 1127–1152.

Hedlin, M. A. H., Alcoverro, B., and D'Spain, G. (**2003**). ''Evaluation of rosette infrasonic noise-reducing spatial filters,'' J. Acoust. Soc. Am. (to be published).

Kaimal, J. C., and Finnigan, J. J. (**1994**). *Atmospheric Boundary Layer Flows: Their Structure and Measurement* (Oxford University Press, Oxford).

McDonald, J. A., Douze, E. J., and Herrin, E. (**1971**). ''Structure of Atmospheric Turbulence,'' Geophys. J. R. Astron. Soc. **26**, 99–109.

Morgan, S., and Raspet, R. (**1992**). ''Investigation of the mechanisms of low-frequency wind noise generation outdoors,'' J. Acoust. Soc. Am. **92**, 1180–1183.

Morgan, M. S. (**1992**). ''An Investigation of the Sources and Attenuation of Wind Noise in Measurement Microphones,'' Ph.D. dissertation, University of Mississippi.

Panofsky, H. A., and Dutton, J. A. (**1984**). *Atmospheric Turbulence: Models and Methods for Engineering Applications* (Wiley, New York).

Phelps, W. (**1938**). ''Microphone wind screening,'' RCA Rev. **3**, 203–212.

Priestley, J. T. (**1966**). ''Correlation studies of pressure fluctuations on the ground beneath a turbulent boundary layer,'' NBS Report 8942, U.S. Dept. of Commerce, National Bureau of Standards.

Schomer, P. D., Raspet, R., Brunner, J., Marshal, D., Wagner, M., and Walker, D. (**1990**). ''Reduction of wind noise for unattended blast noise monitoring,'' Noise Control Eng. J. **34**(2), 77–88.

Strasberg, M. (**1979**). ''Nonacoustic noise interference in measurements of infrasonic ambient noise,'' J. Acoust. Soc. Am. **66**, 1487–1493.

Strasberg, M. (**1988**). ''Dimensional analysis of windscreen noise,'' J. Acoust. Soc. Am. **83**, 544–548.